Simulations of the Morphology of Cylinder-Forming Asymmetric Diblock Copolymer Thin Films on Nanopatterned Substrates

Qiang Wang,† Paul F. Nealey, and Juan J. de Pablo*

Department of Chemical Engineering, University of Wisconsin−Madison, Madison, Wisconsin 53706-1691

Received June 24, 2002

ABSTRACT: We report a first study on the use of chemically nanopatterned substrates to induce long-range ordering (in the plane of the film) of perpendicular cylinders confined between the substrate and an upper homogeneous surface. Two conditions are essential for obtaining the long-range ordering: a lower hexagonally patterned substrate, commensurate with perpendicular cylinders having the same dimensions and packing as in the bulk, and an upper neutral or weakly preferential surface for the longer blocks. By examining the spatial fluctuations of perpendicular cylinders, we propose that combining nanopatterned substrates with electric fields perpendicular to the film could reach the ultimate goal of producing long-range ordered perpendicular cylinders as templates for nanolithography.

1. Introduction

Block copolymers are known to self-assemble into microphase-separated domains on the length scale of tens of nanometers at temperatures below the order−disorder transition (ODT).[1] In recent years, thin films of block copolymers have received considerable attention because of their potential applications in nanofabrication.[2] Control of morphology in the films, including both the orientation and the ordering of the copolymer microdomains, is essential for such applications. In general, morphologies with the copolymer microdomains (lamellae or cylinders) oriented perpendicular to a substrate are desirable. Such morphologies can be obtained by finely tuning the surface−block interactions and the film thickness[3−22] or by applying electric fields perpendicular to the film.[18,23−26] Unfortunately, the perpendicular structures obtained on homogeneous substrates are devoid of long-range ordering in the plane of the film; grains with typical sizes of a few hundreds of nanometers can be clearly seen in experiments.[3−5,18] To obtain well-ordered perpendicular structures over microns or even larger distances, one strategy is to register the microdomains with chemically nanopatterned substrates.[27−36] In the case of lamellar structures, the feasibility of employing stripe-patterned substrates has been demonstrated experimentally;[27−29] our recent Monte Carlo simulations and theoretical calculations[30,31] are consistent with the available experimental evidence.

For applications in nanofabrication, however, cylindrical structures are likely to have a much wider impact. Such structures have potential for production of nanowires, high-density storage devices, molecular electronics, etc. To the best of our knowledge, the use of nanopatterned substrates has not been considered before (either experimentally or theoretically) as a means to induce long-range ordering in thin films of cylinder-forming asymmetric diblock copolymers. Therefore, in this work we report results of Monte Carlo simulations on the morphology of cylinder-forming asymmetric diblock copolymers on chemically nanopatterned substrates. Our purpose is to arrive at optimal experimental conditions to use such substrates to improve the long-range ordering of perpendicular cylinders.

The morphology of block copolymers can be studied using a number of theoretical or numerical formalisms.[13,21,31,37−39] In this initial, exploratory work, we choose to use Monte Carlo simulations to avoid some of the assumptions implicit in theoretical work. While simulations of this nature would have not been possible in the past, the advent of recent simulation methods[40] has allowed us to investigate the structure and properties of confined polymeric systems with confidence. Note that, for applications in nanolithography, low-molecular-weight polymers are necessary to reach the target length scale of a few tens of nanometers; molecular simulations can provide accurate predictions for such systems.

Mean-field theory predicts that cylinders of diblock copolymers are regular-hexagonally packed at a characteristic intercylinder distance L_0 that minimizes the free energy of the system.[41,42] In these systems, however, fluctuations can be important; our simulations show that individual cylinders actually fluctuate around their average packing positions. Such spatial fluctuations are related to the lack of long-range ordering of perpendicular cylinders on homogeneous substrates. In our simulations we also examine the spatial fluctuations of perpendicular cylinders on various substrates. To the best of our knowledge, this is so far the only simulation study addressing the issue of spatial fluctuations in confined copolymer films.

This paper is organized as follows: In section 2 we briefly describe the model and the simulation methodology. In section 3 we present thin-film morphologies observed on various nanopatterned substrates, including hexagonally patterned substrates, stripe-patterned substrates, and a square-patterned substrate. In section 4 we present our methods and results for the spatial fluctuations of perpendicular cylinders on different substrates. The last section is devoted to conclusions.

2. Model

Our Monte Carlo simulations are performed in an expanded grand-canonical ensemble in the framework

† Current address: Department of Chemical Engineering and the Materials Research Laboratory, University of California−Santa Barbara, Santa Barbara, CA 93106.

* To whom correspondence should be addressed.

10.1021/ma020996t CCC: $25.00
Published on Web 02/07/2003

of a simple cubic lattice. The model employed here is the same as that employed in refs 9, 19, and 30, where detailed descriptions can be found. Only a brief account is given here.

2.1. Simple Cubic Lattice Model. In the simple cubic lattice model, an asymmetric diblock copolymer chain consists of N segments. The first N_A segments are of type A, and the rest are of type B. Each segment occupies one lattice site, and each lattice site is occupied by at most one segment. A rectangular simulation box of dimensions $L_x \times L_y \times L_z$ is employed. To simulate a confined film, two flat surfaces are introduced through two additional layers of lattice sites at $z = 0$ and $z = L_z + 1$, respectively. To represent hard surfaces, these lattice sites are not allowed to be occupied by polymer segments. Diblock copolymers are therefore confined to a thin-film geometry of thickness $D = L_z - 1$. Periodic boundary conditions (PBC) are imposed in the x and y directions.

In our model, we only consider repulsions between nonbonded nearest-neighbor A−B pairs separated by one lattice unit ($\epsilon_{A-B} > 0$), and we set $\epsilon_{A-A} = \epsilon_{B-B} = 0$. Any interactions involving vacancies (unoccupied lattice sites) are also set to zero. The upper surface is homogeneous, consisting of only sH sites. We set $\epsilon_{sH-A} \geq 0$, $\epsilon_{sH-B} \geq 0$, and $\epsilon_{sH-A}\epsilon_{sH-B} = 0$ (that is, at least one of these two parameters is set to 0). We characterize the surface preference by $\alpha_H \equiv (\epsilon_{sH-B} - \epsilon_{sH-A})/\epsilon_{A-B}$. Therefore, when $\alpha_H > 0$, the upper surface repels B and thus prefers A segments, and vice versa. According to our previous work,[9,19,30,31] $|\alpha_H| = 0.5$ corresponds to a weakly preferential surface, and $|\alpha_H| = 2$ corresponds to a strongly preferential surface. Three kinds of sites populate the lower surface (substrate): sA, sB, and sC, whose nature depends on their interactions with the two blocks of the copolymers. We set $\epsilon_{sA-A} = \epsilon_{sB-B} = 0$ and $\epsilon_{sA-B} = \epsilon_{sB-A} = 2\epsilon_{A-B}$; the sA sites strongly repel B segments and therefore prefer A segments, and vice versa. The nature of sC sites is similar to that of sH sites, with $\alpha_C \equiv (\epsilon_{sC-B} - \epsilon_{sC-A})/\epsilon_{A-B}$ characterizing their preference. If $\alpha_C = -2$, the sC sites are equivalent to sB sites.

2.2. Simulations in an Expanded Grand-Canonical Ensemble. We perform Monte Carlo simulations in a variant of the expanded grand-canonical ensemble method proposed by Escobedo and de Pablo.[43] The chemical potential and temperature of the simulated system are specified prior to a simulation; the confined copolymers are therefore in thermodynamic equilibrium with a bulk phase having the same chemical potential and temperature, and the density of the system is allowed to fluctuate during the simulation. In addition to molecule displacements by reptation moves and local (kink-jump and crankshaft) moves, we employ growing/shrinking moves to gradually insert/remove copolymer chains from the system.[9] These moves are performed with m_A segments of type A and, simultaneously, m_B segments of type B. To preserve a constant composition of the asymmetric diblock copolymers, defined as $f_A \equiv N_A/N$, we require $m_A/(m_A + m_B) = f_A$. To facilitate transitions, configurational bias is used for these growing/shrinking moves.[9] Metropolis-like acceptance criteria are used in our simulations. One Monte Carlo step (MCS) consists of $0.7 \times L_x \times L_y \times L_z$ trials of reptation, local, and growing/shrinking moves, each of which occurs with the same probability of $^1/_3$. In general, we discard the first 5×10^5 MCS (or more) for equilibration and then make a run of at least 2×10^6 MCS while collecting data every 5 MCS.

As in our previous work,[19] we study asymmetric diblock copolymers with $N = 36$ and $f_A = {}^1/_4$. We set the reduced temperature to be $T^* \equiv k_B T/\epsilon_{A-B} = 1.5$, where k_B is Boltzmann's constant and T is the absolute temperature. We also set the reduced chemical potential at $\mu^* \equiv \mu/(k_B T) = 46$, where μ is the chemical potential of the copolymer chain. Under these conditions, the asymmetric diblock copolymers form hexagonally packed cylinders in the bulk, with a diameter of about 9, an intercylinder distance $L_0 \approx 16.8$, and a distance across two (staggered) layers of cylinders $L_2 \approx 28.1$ (in units of lattice spacing).[19] (The ODT temperature of our system is estimated to be around $T^* = 3.0$ at this chemical potential; our simulations are therefore in the intermediate segregation regime.) These conditions also lead to densities (fraction of occupied lattice sites) of about 0.7, representing highly concentrated copolymer solutions or melts.[44] We use $m_A = 1$, which leads to an acceptance rate of about 40% for our growing/shrinking moves.[19]

2.3. Substrate Patterns. As shown in Figure 1, three types of substrate pattern are considered in this work: hexagonal pattern, stripe pattern, and square pattern. For the hexagonal pattern, the yellow regions in Figure 1a consist of sA sites, the blue regions consist of sB sites, and the rest are sC sites. In the case of lamellae-forming symmetric diblock copolymers, it has been shown that a substrate pattern commensurate with the bulk structure is essential to obtain long-range ordered perpendicular lamellae.[27−35] Therefore, here we set the hexagonal pattern as $w_{sx} = 7$, $w_{sy} = 8$, and $\theta = \arctan(7/4) \approx 60.26°$, which are defined in Figure 1a; this makes the pattern commensurate with perpendicular cylinders having bulk characteristic dimensions and packing in the framework of our lattice model.

For the stripe pattern, the blue regions in Figure 1b consist of sB sites, and the rest are sC sites. Such chemically stripe-patterned substrates can actually be created by extreme ultraviolet interferometric lithography (EUV-IL),[28,45] where the stripe preference can be adjusted by controlling the exposure dose.[46] By double exposure at an angle of 120° with EUV-IL, or by EUV-IL with two Lloyd's mirrors arranged at 120°, the aforementioned hexagonally patterned substrates can also be created.[47]

For the square pattern, the yellow regions in Figure 1c consist of sA sites, and the rest are sB sites. We set $w_{sx} = w_{sy} = 8$ so that the sA regions are commensurate with perpendicular cylinders having bulk characteristic dimensions. Such a substrate can be obtained in a manner similar to that employed for hexagonally patterned substrates, with an angle of 90° instead.

2.4. Characterization of Morphology. To identify a morphology in simulations of confined films, in addition to visual inspection of system configurations (snapshots), we also calculate the following ensemble-averaged profiles. These profiles are more meaningful and conclusive for characterization of various morphologies than visual inspection of a few snapshots.[9,19,30]

The two-dimensional order parameter profile can be defined as $\psi(x,y) \equiv \langle \rho_A(x,y) - \rho_B(x,y) \rangle$, where $\rho_A(x,y)$, for example, is the fraction of lattice sites occupied by the A segments at a given (x,y), and $\langle\ \rangle$ represents the average over other directions (the z direction in this case) for each collected configuration and then over all

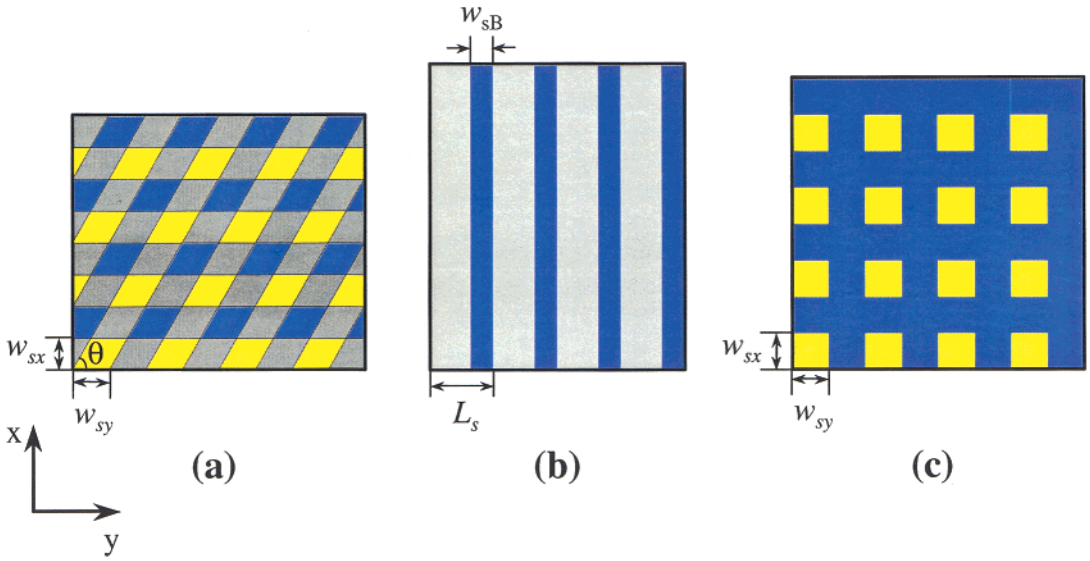

Figure 1. Chemically nanopatterned substrates: (a) Hexagonally patterned substrate, where the yellow regions consist of sA sites strongly preferring the shorter (A) blocks, the blue regions consist of sB sites strongly preferring the longer (B) blocks, and the rest are sC sites. We set $w_{sx} = 7$, $w_{sy} = 8$, and $\theta = \arctan(7/4) \approx 60.26°$, so that the hexagonal pattern is commensurate with perpendicular cylinders having bulk characteristic dimensions and packing (in the framework of a cubic lattice model). (b) Stripe-patterned substrate, where the blue regions are sB sites, and the rest are sC sites. (c) Square-patterned substrate, where the yellow regions are sA sites, and the rest are sB sites. We set $w_{sx} = w_{sy} = 8$. Periodic boundary conditions are applied along the x and y directions in all cases.

Table 1. Values of $\sigma(x,y,z)$ Used in Calculating Pattern Index Profiles

		segment at (x,y,z)		
	$\sigma(x,y,z)$	vacancy	A	B
substrate site at (x,y)	sA	0	1	−1
	sB or sC ($\alpha_C = -2$)	0	−1	1
	sC ($\alpha_C = 0$)	0	0	0

collected configurations (at equilibrium). We can also define $\psi(y,z)$ and $\psi(x,z)$ in a similar way.

As in our previous work,[9,19,30,31] the one-dimensional order parameter profile is defined as $\psi(z) \equiv \langle \rho_A(z) - \rho_B(z) \rangle$, where $\rho_A(z)$, for example, is the fraction of lattice sites occupied by the A segments in the cross section of the $x-y$ plane at a given z. For our systems, the maximum (minimum) value of the order parameter profiles is about 0.7 (−0.7), corresponding to the A-rich (B-rich) domains.

As in our previous work,[30] we also define the pattern index profile $P(z)$ as

$$P(z) \equiv \left\langle \frac{1}{L_x L_y} \sum_{x=1}^{L_x} \sum_{y=1}^{L_y} \sigma(x,y,z) \right\rangle$$

where the values of $\sigma(x,y,z)$ are listed in Table 1. If the pattern in the $x-y$ cross section is completely in-phase with the substrate pattern, then $P(z) \approx 0.7$. Similarly, if the pattern in the cross section is completely out-of-phase with the substrate pattern, then $P(z) \approx -0.7$.

3. Morphology on Nanopatterned Substrates

3.1. Hexagonally Patterned Substrates. In this section we use a box size of $L_x = 56$ ($2L_2$) and $L_y = 64$ ($4L_0$). Since we set the hexagonal pattern of the substrate to be commensurate with perpendicular cylinders having bulk characteristic dimensions and packing, sC sites repelling the shorter (A) blocks (e.g., $\alpha_C = -2$) are suitable for inducing the desirable perpendicular cylinders. According to our previous work on thin-film morphology of cylinder-forming asymmetric diblock copolymers between two homogeneous surfaces, an energetically neutral upper surface ($\alpha_H = 0$) exhibits a slight preference for the shorter blocks (due to the enrichment of chain ends near hard surfaces); a surface with $\alpha_H = -0.2$ is "effectively neutral" and is ideal for the formation of perpendicular cylinders.[19] Figure 2 therefore shows the 2D order parameter profiles for the case of $\alpha_C = -2$, $\alpha_H = -0.2$, and $D = 84$ ($3L_2$); we see that perpendicular cylinders form throughout the entire film and are registered with the substrate pattern. We have observed the same morphology for other film thicknesses under similar conditions. Such a hexagonally patterned substrate can be used to induce the long-range ordering of perpendicular cylinders. Note that, although the sA regions on the substrate are rhombic, the A-rich domains in the film are still circular. This implies that the detailed shape of the sA regions is not crucial; instead, the hexagonal arrangement of these regions is more important for inducing the long-range ordering of perpendicular cylinders.

Consistent with our previous results,[19] if α_H deviates from the "effectively neutral" condition too much, parallel structures (cylinders or lamellae) form near the upper surface. Figure 3 shows a representative configuration for the case of $\alpha_C = -2$, $\alpha_H = 0.5$, and $D = 28$ (L_2); the morphology consists of perpendicular cylinders registered with the substrate pattern in the lower part of the film ($z = 1-11$), one layer of parallel cylinders formed by connecting the perpendicular cylinders in the middle of the film ($z = 12-23$), and one A−B lamella having a planar A−B interface parallel to the surfaces in the upper part of the film ($z = 24-29$). The morphology for the case of $\alpha_H = -1$ is similar, except that the A−B lamella is not seen. This is consistent with our previous results that the surface-induced parallel lamella is not observed near a surface preferring the longer (B) blocks. Figure 4 shows the 1D order parameter profiles and the pattern index profiles for these two cases. For thicker films, more than one layer of parallel cylinders is observed.

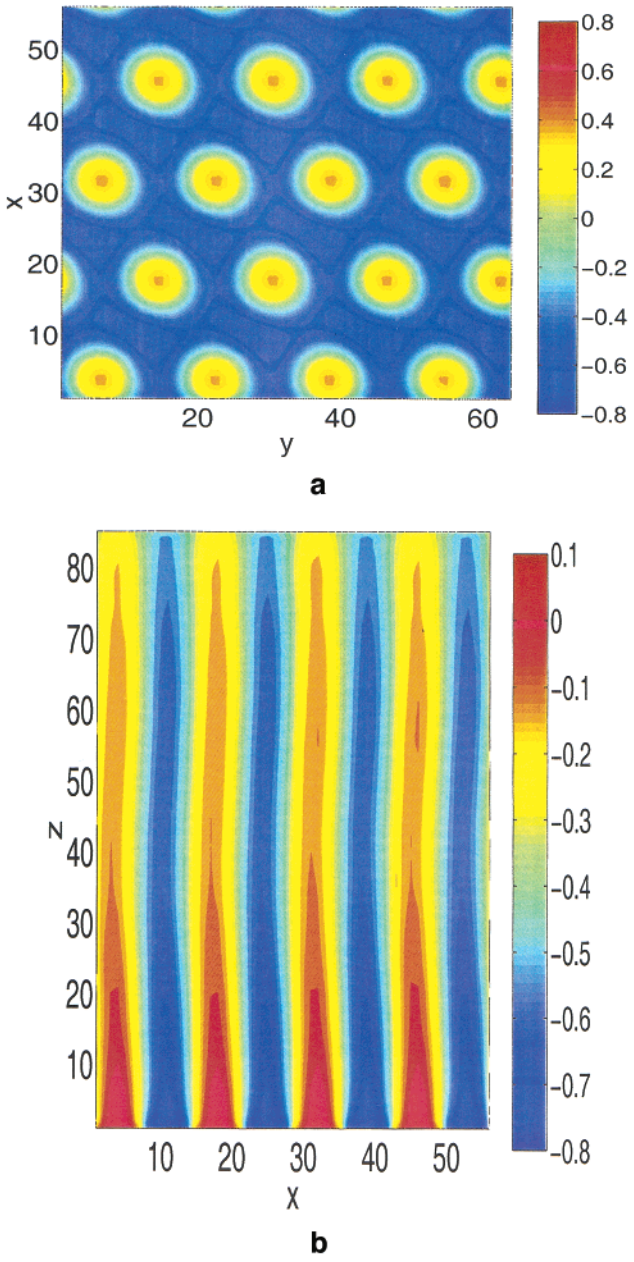

Figure 2. Two-dimensional order parameter profiles for the morphology between a lower hexagonally patterned substrate ($\alpha_C = -2$) and an upper "effectively neutral" surface ($\alpha_H = -0.2$). The color bar in each graph gives the correspondence of different colors to the value of the two-dimensional order parameter. The box size is 56 × 64 × 85. Perpendicular cylinders registered with the substrate pattern form throughout the entire film.

If the hexagonally patterned substrate is produced by double exposure, the sC sites are in general not equivalent to sB sites. Figure 5 shows a representative configuration for the case of $\alpha_C = \alpha_H = 0$ and $D = 28$ (L_2). Because of the slight preference of the neutral sC sites for the shorter blocks (as noted above), one layer of half-cylinders parallel to the substrate forms along the y direction in the lower part of the film ($z = 1-7$). This is also clearly seen in Figure 6, where the 2D order parameter profiles are shown. Note that the period of these half-cylinders is 14, set by the substrate pattern. As shown in Figure 5, one layer of perforated lamellae forms in the middle of the film ($z = 8-22$), and another layer of a labyrinthine-type morphology forms in the upper part of the film ($z = 23-29$). The formation of this complex parallel morphology is mainly due to the neutral sC sites on the substrate; perpendicular cylinders similar to those shown in Figure 2 are observed when $\alpha_C = -2$. Figure 7 shows the 1D order parameter profiles and the pattern index profiles for these two cases. The parallel morphology is evident from the large variation of $\psi(z)$ in the case $\alpha_C = 0$, and the perpendicular cylinders registered with the substrate pattern are seen from the values of $\psi(z)$ and $P(z)$ in the case $\alpha_C = -2$.

3.2. Stripe-Patterned Substrates. In this section we use a box size of $L_x = 67$ ($4L_0$) and fix the film thickness to be $D = 28$ (L_2). To induce *perpendicular* cylinders with stripe-patterned substrates, we set the stripe pattern to be commensurate with bulk cylinders, that is, the stripe pattern period $L_s = 14$ ($L_2/2$) and therefore $L_y = 56$ ($2L_2$). We also set $\alpha_C = \alpha_H = -0.2$, so that perpendicular cylinders form on the sC stripes and persist throughout the entire film. Figure 8 shows the 2D order parameter profiles for the case where the width of the sB stripes is $w_{sB} = 5$. Note that, due to the translational symmetry in the x direction, perpendicular cylinders move along this direction during the course of a simulation run; the $\psi(x, y)$ shown in Figure 8 is therefore an "aligned" order parameter profile[48] obtained by deducting the movement of cylinders along the x direction. Since all perpendicular cylinders form on the sC stripes, we expect that such a stripe-patterned substrate can induce in-plane ordering of perpendicular cylinders over a longer range than that obtained by the use of a homogeneous substrate.

The diameter of the bulk cylinders is about 9;[19] $w_{sB} = 5$ therefore matches perpendicular cylinders having bulk characteristic dimensions. Interestingly, perpendicular cylinders similar to those shown in Figure 8 can be obtained over a wide range of w_{sB}; Figure 9 shows the 1D order parameter profiles for different w_{sB} with

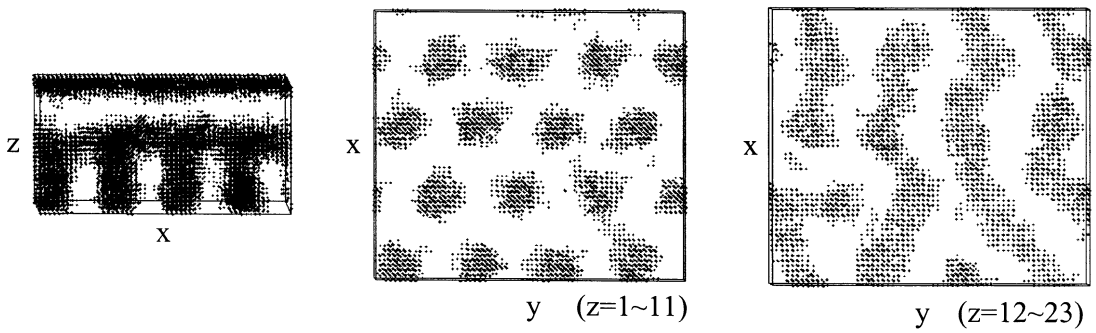

Figure 3. Representative configuration of the morphology between a lower hexagonally patterned substrate ($\alpha_C = -2$) and an upper preferential surface for the A blocks ($\alpha_H = 0.5$). Only A segments are shown as dots. The box size is 56 × 64 × 29.

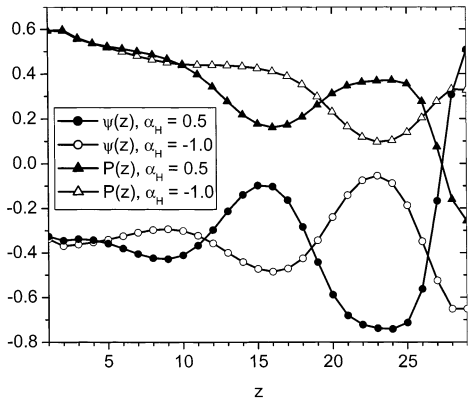

Figure 4. One-dimensional order parameter profiles and the pattern index profiles for morphologies between a lower hexagonally patterned substrate ($\alpha_C = -2$) and an upper preferential surface. The box size is 56 × 64 × 29.

$\alpha_C = -0.2$; perpendicular cylinders are obtained in all cases.

In contrast, only a narrow range of α_C is available for obtaining such perpendicular cylinders. Figure 10 shows the 1D order parameter profiles for different α_C with $w_{sB} = 5$; perpendicular cylinders are obtained only in the cases where the sC stripes are close to the "effectively neutral" condition, that is, where $\alpha_C = 0$, -0.2, and -0.5. In the case $\alpha_C = -1$, two layers of parallel cylinders are observed; a representative configuration is shown in Figure 11. The intercylinder distance of these parallel cylinders is 16.05, closer to L_0 than L_s; the stripe pattern on the substrate is therefore ignored by the copolymers. A similar morphology was observed in our previous work, where the copolymers were confined between two homogeneous and identical surfaces with $\alpha_H = -0.5$.[19] In the case $\alpha_C = 0.5$, one layer of half-cylinders parallel to the substrate forms along the x direction in the lower part of the film ($z = 1-7$). These half-cylinders comply with the stripe pattern on the substrate and therefore have an intercylinder distance of 14. For even stronger preference of the sC stripes for the A blocks, e.g. $\alpha_C = 1$, another layer of parallel cylinders forms in the middle of the film ($z = 8-21$); this is clearly seen in Figure 12. Since the upper surface is "effectively neutral", perpen-

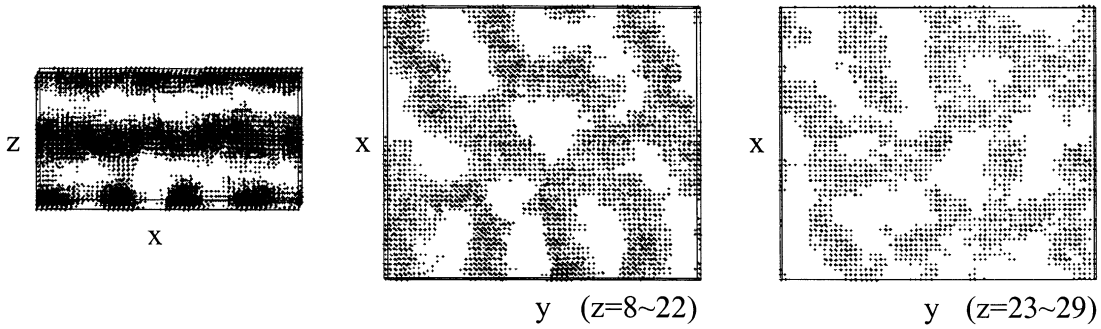

Figure 5. Representative configuration of the morphology between a lower hexagonally patterned substrate ($\alpha_C = 0$) and an upper neutral surface ($\alpha_H = 0$). Only A segments are shown as dots. The box size is 56 × 64 × 29.

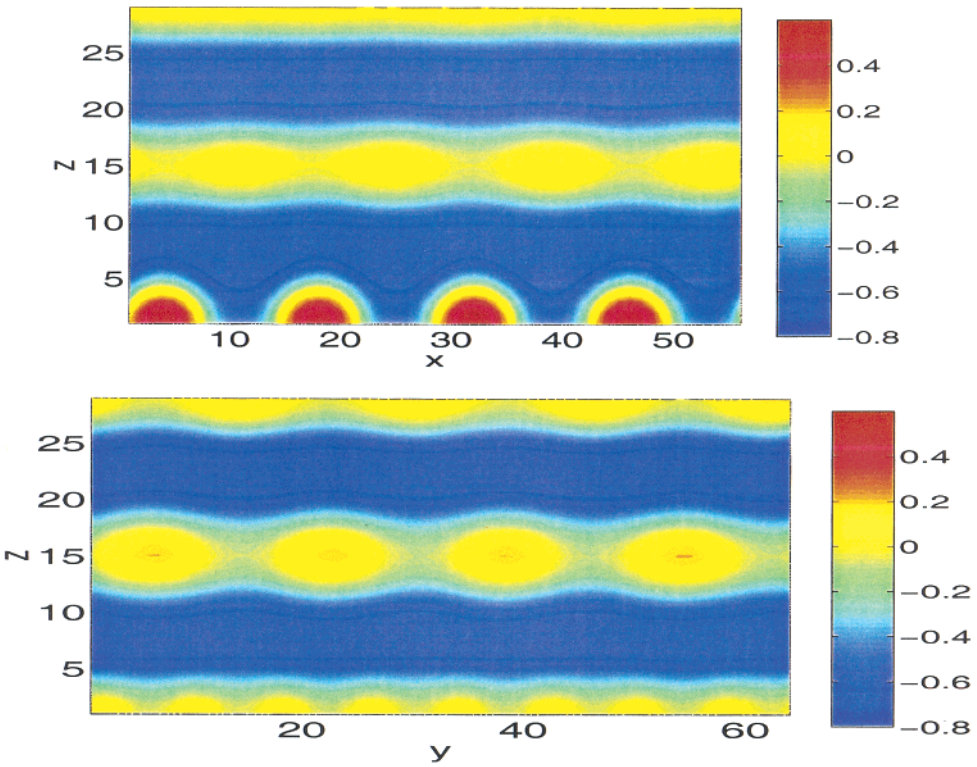

Figure 6. Two-dimensional order parameter profiles for the morphology between a lower hexagonally patterned substrate ($\alpha_C = 0$) and an upper neutral surface ($\alpha_H = 0$). The color bar in each graph gives the correspondence of different colors to the value of the two-dimensional order parameter. The box size is 56 × 64 × 29.

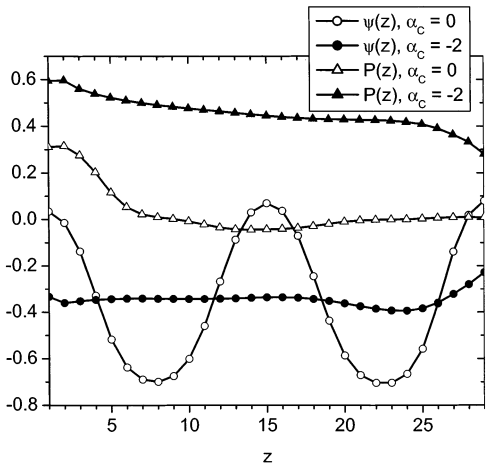

Figure 7. One-dimensional order parameter profiles and the pattern index profiles for morphologies between a lower hexagonally patterned substrate and an upper neutral surface ($\alpha_H = 0$). The box size is 56 × 64 × 29.

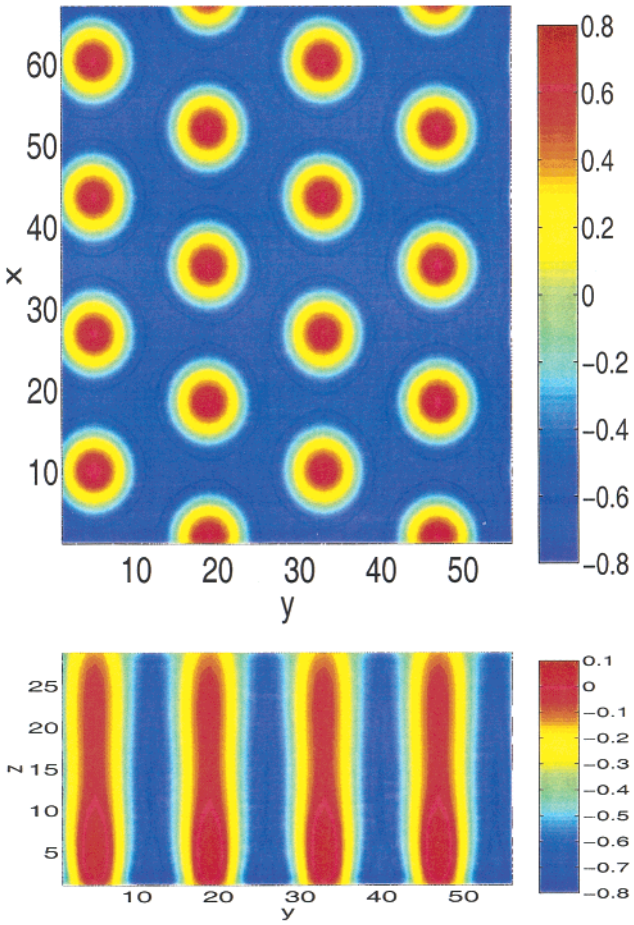

Figure 8. Two-dimensional order parameter profiles for the morphology between a lower stripe-patterned substrate (L_s = 14, w_{sB} = 5, and $\alpha_C = -0.2$) and an upper "effectively" neutral surface ($\alpha_H = -0.2$). The color bar in each graph gives the correspondence of different colors to the value of the two-dimensional order parameter. $\psi(x,y)$ is "aligned" along the x direction. The box size is 67 × 56 × 29. Perpendicular cylinders registered with the substrate pattern form throughout the entire film.

dicular cylinders form in the upper part of the film (z = 22−29). These perpendicular cylinders correspond to the circles seen in $\psi(x,y)$, which is also an "aligned" order parameter profile.

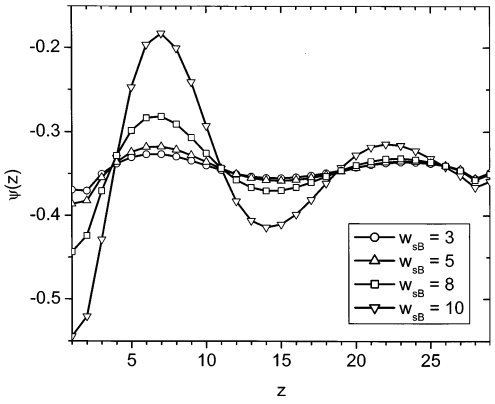

Figure 9. One-dimensional order parameter profiles for morphologies between a lower stripe-patterned substrate (L_s = 14 and $\alpha_C = -0.2$) and an upper "effectively" neutral surface ($\alpha_H = -0.2$). The box size is 67 × 56 × 29. Perpendicular cylinders are obtained in all cases.

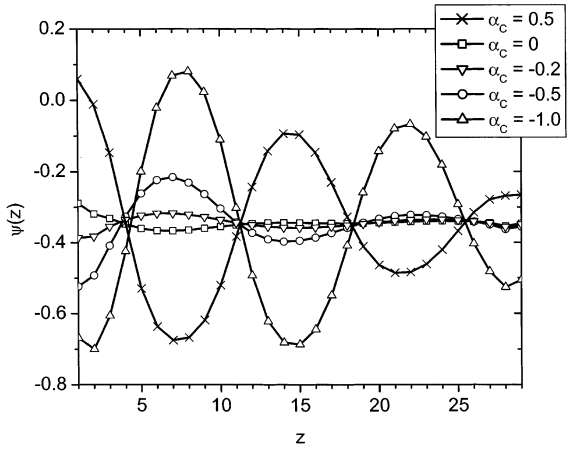

Figure 10. One-dimensional order parameter profiles for morphologies between a lower stripe-patterned substrate (L_s = 14 and w_{sB} = 5) and an upper "effectively" neutral surface ($\alpha_H = -0.2$). The box size is 67 × 56 × 29. Perpendicular cylinders are obtained only in the cases of α_C = 0, −0.2, and −0.5.

To obtain *parallel* cylinders having bulk dimensions, we set L_s = 17 and therefore L_y = 51 ($3L_0$). We also set w_{sB} = 8, α_C = 2, and α_H = 0. Figure 13 clearly shows that we have parallel cylinders registered with the stripe pattern on the substrate in this case. The formation of half-cylinders near the upper neutral surface is consistent with our previous work.[19]

3.3. Square-Patterned Substrate. In this section we use a box size of 64 × 64 × 29 and set $\alpha_H = -0.2$. Since the square pattern on the substrate is commensurate with the dimensions of bulk cylinders but not their hexagonal packing, perpendicular cylinders complying with the square pattern are only obtained near the substrate (z = 1−5). This can be seen in both Figures 14 and 15. Further away from the substrate, the cylinders rearrange themselves to recover their bulk hexagonal packing. One way of doing this is for adjacent layers of cylinders to slide along the y direction and to develop a staggered packing; as shown in Figure 14, the square packing of cylinders is thereby gradually transformed into a hexagonal packing as z increases. This is why in Figure 15 the perpendicular cylinders disappear from $\psi(y,z)$ as z increases. Note that the hexagon formed in this way is not a regular hexagon; it is stretched along the x direction. The cylinders therefore also bend in the x direction to reduce this stretching. From $\psi(x,z)$ in

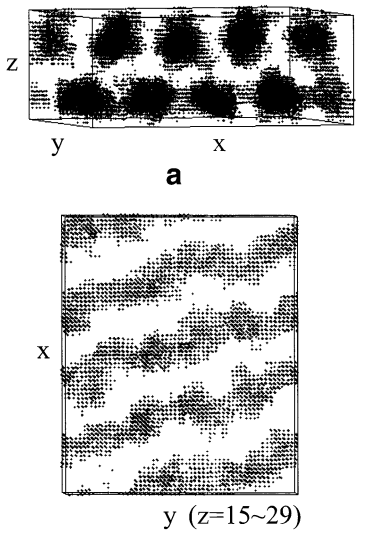

Figure 11. Representative configuration of the morphology between a lower stripe-patterned substrate ($L_s = 14$, $w_{sB} = 5$, and $\alpha_C = -1$) and an upper "effectively" neutral surface ($\alpha_H = -0.2$). Only A segments are shown as dots. The box size is 67 × 56 × 29.

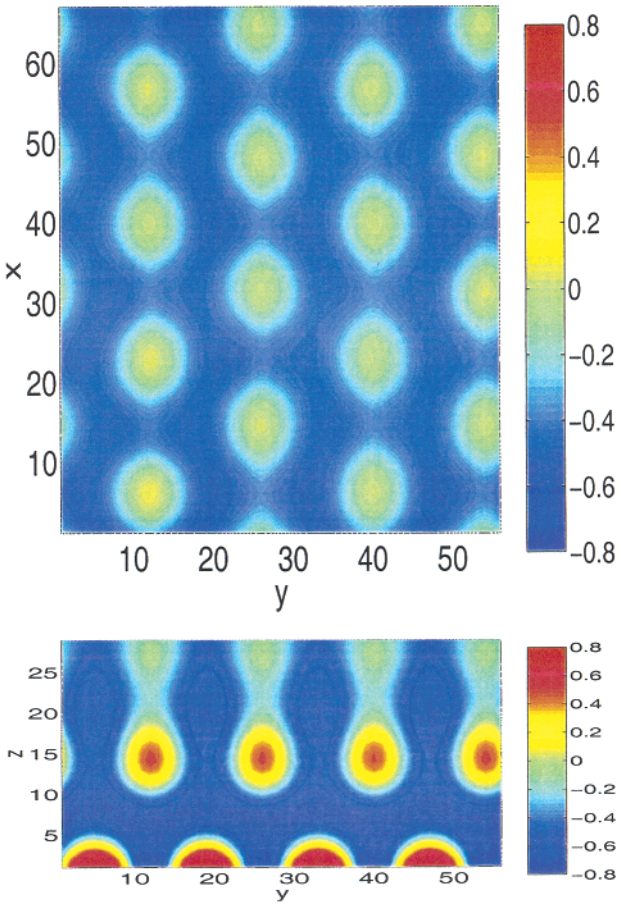

Figure 12. Two-dimensional order parameter profiles for the morphology between a lower stripe-patterned substrate ($L_s = 14$, $w_{sB} = 5$, and $\alpha_C = 1$) and an upper "effectively" neutral surface ($\alpha_H = -0.2$). The color bar in each graph gives the correspondence of different colors to the value of the two-dimensional order parameter. $\psi(x,y)$ is "aligned" along the x direction. The box size is 67 × 56 × 29.

Figure 15, we measure in the middle of the film the angle between the cylinder axis and the z axis to be around 15°, smaller than the 30° required to form a regular-hexagonal array of cylinders (with an intercylinder distance of 16). In the vicinity of the upper surface, the cylinders are perpendicular to the surface. This bending of cylinders is reminiscent of the undulated perpendicular lamellae studied in our previous work, where the lamellae were confined between an upper neutral surface and a lower stripe-patterned substrate with a pattern period larger than the bulk lamellar period.[31]

This case demonstrates the importance of using a nanopatterned substrate having a pattern commensurate with the bulk morphology of block copolymers, if the substrate pattern is to propagate throughout the entire film.

4. Spatial Fluctuations of Perpendicular Cylinders

In this section we examine the spatial fluctuations of perpendicular cylinders on different substrates, namely, a homogeneous substrate, a stripe-patterned substrate, and a hexagonally patterned substrate. To form perpendicular cylinders in the film, in all cases we set the upper homogeneous surface to be "effectively neutral" ($\alpha_H = -0.2$). For the homogeneous substrate, we set it to be identical to the upper surface. For the stripe-patterned substrate, we set $L_s = 14$, $w_{sB} = 5$, and $\alpha_C = -0.2$. In contrast to Figure 1b, we now set the stripes to be along the y direction. For the hexagonally patterned substrate we set $\alpha_C = -2$.

Since the periodic boundary conditions imposed in the x and y directions suppress the spatial fluctuations, we use a large box of 112 × 128 × 85, which contains $n = 64$ cylinders oriented perpendicular to the substrate. We number these cylinders by $i = 1, ..., n$, first along the y then along the x direction. We also divide the film evenly into $m = 5$ slices along the z direction and number these slices by $j = 1, ..., m$ along the z direction. For each collected configuration, we calculate the 2D order parameter profile $\psi(x,y;j)$ ($x = 1, ..., L_x$; $y = 1, ..., L_y$) where the average is only taken over the slice j. From the $\psi(x,y;j)$ we then identify the position of cylinder i in slice j, denoted by $\mathbf{r}_{i,j}$, according to the cylinder's center-of-mass in the $x-y$ plane. Here the "mass" at (x,y) is defined as $\max\{\psi(x,y;j), 0\}$. The spatial fluctuations of cylinders can therefore be measured by the deviation of cylindrical packing from the "ideal" case where there are no spatial fluctuations and where all cylinders are at their average packing positions. In a continuum, this "ideal" packing should be a regular hexagon if an appropriate simulation box size $L_x \times L_y$ is chosen. However, since a regular hexagon cannot fit in a lattice model where L_x and L_y must be integers, in our case the "ideal" packing is actually the hexagon represented in Figure 1a. We denote the position of cylinder i in this "ideal" packing by $\mathbf{r}_i^0$. For the simulation box size of 112 × 128, we have $\mathbf{r}_1^0 = (0, 0)^T$, $\mathbf{r}_2^0 = (0, 16)^T$, ..., $\mathbf{r}_9^0 = (8, 8)^T$, ... We then define $\delta(j) \equiv \langle |\mathbf{r}_{i,j} - \mathbf{r}_{1,j} - \mathbf{r}_i^0| \rangle_{i\geq 2}$, where $\langle\ \rangle_{i\geq 2}$ represents the average over cylinders $i = 2, ..., n$ in slice j for each collected configuration and then over all collected configurations (at equilibrium). This quantity measures the spatial fluctuations of perpendicular cylinders.

To circumvent the long ordering process associated with large system sizes, we duplicate according to the periodic boundary conditions a smaller system (56 × 64 × 85) of well-ordered perpendicular cylinders to obtain

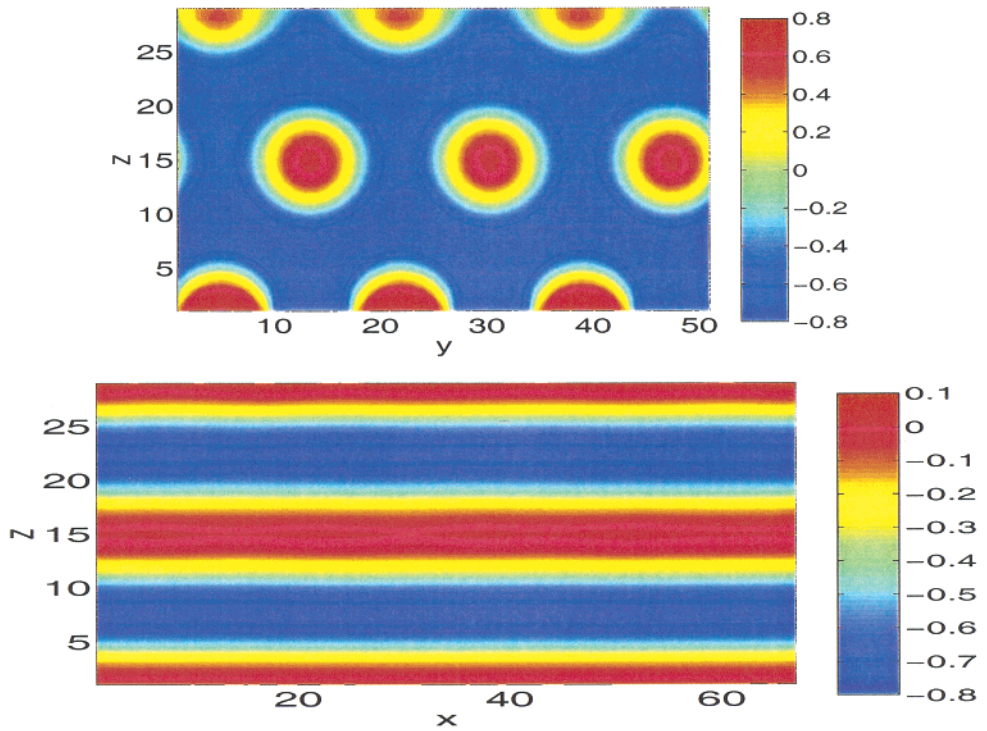

Figure 13. Two-dimensional order parameter profiles for the morphology between a lower stripe-patterned substrate ($L_s = 17$, $w_{sB} = 8$, and $\alpha_C = 2$) and an upper neutral surface ($\alpha_H = 0$). The color bar in each graph gives the correspondence of different colors to the value of the two-dimensional order parameter. The box size is $67 \times 51 \times 29$.

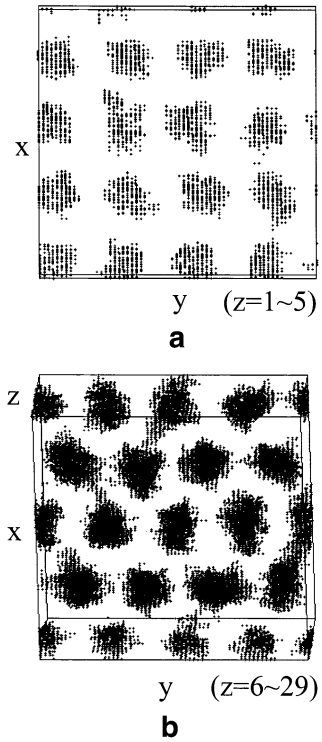

Figure 14. Representative configuration of the morphology between a lower square-patterned substrate and an upper "effectively" neutral surface ($\alpha_H = -0.2$). Only A segments are shown as dots. The box size is $64 \times 64 \times 29$.

the initial configuration. After further equilibration, we conduct a simulation run of 5×10^5 MCS and collect data every 10 MCS. To further reduce the suppression of spatial fluctuations by the periodic boundary conditions, we also employ a box of $228 \times 256 \times 57$ for the hexagonally patterned substrate. In this case, we have $n = 256$ and $m = 3$, and the values of $\mathbf{r}_i^0$ are accordingly different from the above. The initial configuration is prepared from a system of $56 \times 64 \times 57$ of well-ordered perpendicular cylinders, and we conduct a run of 2.5×10^5 MCS to collect data after further equilibration. If we map our simulated system onto an experimental system having $L_0 \approx 30$ nm, this largest system size corresponds to a film of about 100 nm thick with an area of about 0.4 μm $\times$ 0.5 μm.

Our results are shown in Figure 16. We see that the spatial fluctuations of perpendicular cylinders in the first slice, which is closest to the substrate, are largely reduced by the substrate pattern. This explains why nanopatterned substrates can induce long-range ordering of perpendicular cylinders. However, we also see that this reduction of fluctuations does not propagate far into the film. Despite the use of different substrates, all $\delta(j)$ in the interior of the film ($j = 2$, 3, 4 for the box size of $112 \times 128 \times 85$) have about the same value. This is due to the short-range interactions between the substrates and the copolymers. Imposing an electric field perpendicular to the film could propagate the effects of nanopatterned substrates further into the film. Experiments have shown that cylinders of asymmetric diblock copolymers can be aligned along electric field lines due to the different dielectric constants of the two blocks.[18,23,49,50] Note, however, that imposing electric fields perpendicular to the film does not induce the long-range ordering of perpendicular cylinders *in the plane* of the film.

We also see from Figure 16 that, in contrast to nanopatterned substrates, the homogeneous surface seems to slightly increase the spatial fluctuations. Apart from statistical errors, in the case of the homogeneous substrate $\delta(j)$ should be symmetric around $j = 3$, and we also expect $\delta(5)$ to be the same for different substrates due to the large film thickness; we therefore

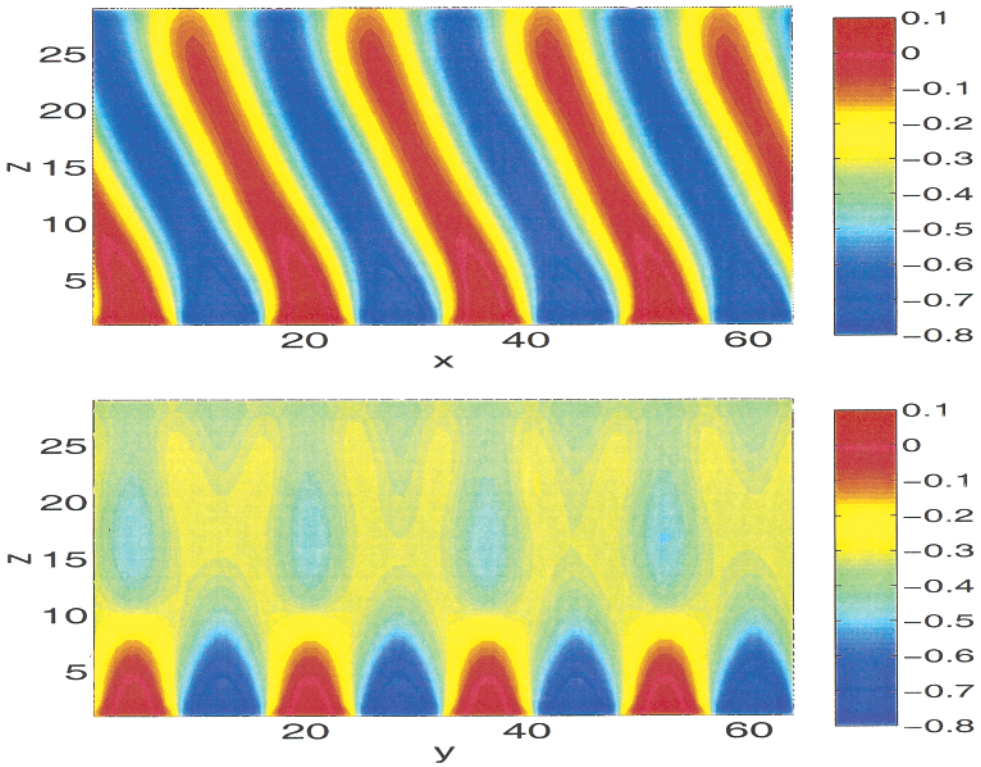

Figure 15. Two-dimensional order parameter profiles for the morphology between a lower square-patterned substrate and an upper "effectively" neutral surface ($\alpha_H = -0.2$). The color bar in each graph gives the correspondence of different colors to the value of the two-dimensional order parameter. The box size is 64 × 64 × 29.

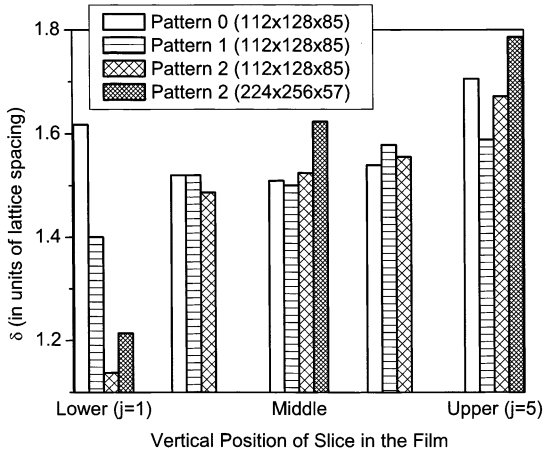

Figure 16. Spatial fluctuations of perpendicular cylinders on various substrates. "Pattern 0" refers to an "effectively neutral" homogeneous substrate ($\alpha_H = -0.2$), "pattern 1" refers to a stripe-patterned substrate ($L_s = 14$, $w_{sB} = 5$, and $\alpha_C = -0.2$), and "pattern 2" refers to a hexagonally patterned substrate ($\alpha_C = -2$). In all cases the upper homogeneous surface is "effectively neutral". The simulation box size is listed in the legend.

estimate the standard deviation of our measured $\delta(j)$ to be 0.05 for the box of 112 × 128 × 85. Longer simulations are needed to obtain more accurate, quantitative results of the spatial fluctuations; the $\delta(j)$ obtained with the box of 228 × 256 × 57, which have smaller statistical errors, confirm the effects of the hexagonally patterned substrate and the homogeneous surface on the spatial fluctuations of perpendicular cylinders. As shown in Figure 16, these $\delta(j)$ are also systematically larger than those obtained with the box of 112 × 128 × 57; this is consistent with the suppression of the spatial fluctuations by the periodic boundary conditions.

5. Conclusions

We have studied the thin-film morphology of cylinder-forming asymmetric diblock copolymers on chemically nanopatterned substrates. Different substrate patterns (hexagonal pattern, stripe pattern, and square pattern), as well as the upper surface preference, are investigated for the purpose of inducing perpendicular cylinders with long-range ordering in the plane of the film. Two conditions are essential for obtaining this morphology suitable for nanolithography: a lower hexagonally patterned substrate, commensurate with perpendicular cylinders having the same dimensions and packing as in the bulk, and an upper neutral or weakly preferential surface for the longer blocks. Using a stripe-patterned substrate, both perpendicular and parallel orientations of the cylinders can be obtained by finely tuning the alternating stripe preference for the two blocks. When the substrate pattern period is commensurate with the bulk periodicity, the cylinders are registered with the stripe pattern. Comparing to the stripe preference, the control of stripe width is less important for obtaining such perpendicular cylinders. In the case of a square-patterned substrate, since the characteristic packing of cylinders in the bulk is a hexagon, the square pattern does not pervade into the film, and the copolymers recover their bulk hexagonal packing after a short distance away from the substrate.

We have also examined the spatial fluctuations of perpendicular cylinders on different substrates (homogeneous, stripe-patterned, and hexagonally patterned substrates). The nanopatterned substrates reduce the spatial fluctuations, thereby inducing the long-range ordering of perpendicular cylinders in the plane of the film. However, because of the short-range interactions between the substrate and the copolymers, this reduction of fluctuations does not propagate far into the film.

We propose that combining nanopatterned substrates with electric fields imposed perpendicular to the film could reach the ultimate goal of producing long-range ordered perpendicular cylinders as templates for nanolithography.

Acknowledgment. Financial support for this work was provided by the Semiconductor Research Corporation through Contract 99-LP-452 and by the NSF, CTS-0210588.

References and Notes

(1) Bates, F. S.; Fredrickson, G. H. *Annu. Rev. Phys. Chem.* **1990**, *41*, 525.
(2) See, for example: (a) Park, M.; Harrison, C.; Chaikin, P. M.; Register, R. A.; Adamson, D. H. *Science* **1997**, *276*, 1401. (b) Hashimoto, T.; Tsutsumi, K.; Funaki, Y. *Langmuir* **1997**, *13*, 6869. (c) Liu, G.; Ding, J.; Hashimoto, T.; Kimishima, K.; Winnik, F. M.; Nigam, S. *Chem. Mater.* **1999**, *11*, 2233. (d) Lammertink, R. G. H.; Hempenius, M. A.; van den Enk, J. E.; Chan, V. Z.-H.; Thomas, E. L.; Vancso, G. J. *Adv. Mater.* **2000**, *12*, 98. (e) Boontongkong, Y.; Cohen, R. E.; Rubner, M. F. *Chem. Mater.* **2000**, *12*, 1628. (f) Peters, R. D.; Yang, X. M.; Wang, Q.; de Pablo, J. J.; Nealey, P. F. *J. Vac. Sci. Technol. B* **2000**, *18*, 3530. (g) Thurn-Albrecht, T.; Schotter, J.; Kastle, G. A.; Emley, N.; Shibauchi, T.; Krusin-Elbaum, L.; Guarini, K.; Black, C. T.; Tuominen, M. T.; Russell, T. P. *Science* **2000**, *290*, 2126.
(3) Kellogg, G. J.; Walton, D. G.; Mayes, A. M.; Lambooy, P.; Russell, T. P.; Gallagher, P. D.; Satija, S. K. *Phys. Rev. Lett.* **1996**, *76*, 2503.
(4) Koneripalli, N.; Levicky, R.; Bates, F. S.; Ankner, J.; Kaiser, H.; Satija, S. K. *Langmuir* **1996**, *12*, 6681.
(5) Huang, E.; Russell, T. P.; Harrison, C.; Chaikin, P. M.; Register, R. A.; Hawker, C. J.; Mays, J. *Macromolecules* **1998**, *31*, 7641.
(6) Kikuchi, M.; Binder, K. *J. Chem. Phys.* **1994**, *101*, 3367.
(7) Sommer, J. U.; Hoffmann, A.; Blumen, A. *J. Chem. Phys.* **1999**, *111*, 3728.
(8) Geisinger, T.; Muller, M.; Binder, K. *J. Chem. Phys.* **1999**, *111*, 5241.
(9) Wang, Q.; Yan, Q.; Nealey, P. F.; de Pablo, J. J. *J. Chem. Phys.* **2000**, *112*, 450.
(10) Walton, D. G.; Kellogg, G. J.; Mayes, A. M.; Lambooy, P.; Russell, T. P. *Macromolecules* **1994**, *27*, 6225.
(11) Brown, G.; Chakrabarti, A. *J. Chem. Phys.* **1995**, *102*, 1440.
(12) Turner, M. S.; Johner, A.; Joanny, J.-F. *J. Phys. I* **1995**, *5*, 917.
(13) Matsen, M. W. *J. Chem. Phys.* **1997**, *106*, 7781.
(14) Pickett, G. T.; Balazs, A. C. *Macromolecules* **1997**, *30*, 3097.
(15) Tang, W. H. *Macromolecules* **2000**, *33*, 1370.
(16) Fasolka, M. J.; Banerjee, P.; Mayes, A. M.; Pickett, G.; Balazs, A. C. *Macromolecules* **2000**, *33*, 5702.
(17) Tsori, Y.; Andelman, D. *Eur. Phys. J. E* **2001**, *5*, 605.
(18) Thurn-Albrecht, T.; Steiner, R.; DeRouchey, J.; Stafford, C. M.; Huang, E.; Bal, M.; Tuominen, M.; Hawker, C. J.; Russell, T. P. *Adv. Mater.* **2000**, *12*, 787.
(19) Wang, Q.; Nealey, P. F.; de Pablo, J. J. *Macromolecules* **2001**, *34*, 3458.
(20) Suh, K. Y.; Kim, Y. S.; Lee, H. H. *J. Chem. Phys.* **1998**, *108*, 1253.
(21) Huinink, H. P.; Brokken-Zijp, J. C. M.; van Dijk, M. A.; Sevink, G. J. A. *J. Chem. Phys.* **2000**, *112*, 2452.
(22) Huinink, H. P.; van Dijk, M. A.; Brokken-Zijp, J. C. M.; Sevink, G. J. A. *Macromolecules* **2001**, *34*, 5325.
(23) Thurn-Albrecht, T.; DeRouchey, J.; Russell, T. P.; Jaeger, H. M. *Macromolecules* **2000**, *33*, 3250.
(24) Pereira, G. G.; Williams, D. R. M. *Macromolecules* **1999**, *32*, 8115.
(25) Ashok, B.; Muthukumar, M.; Russell, T. P. *J. Chem. Phys.* **2001**, *115*, 1559.
(26) Tsori, Y.; Andelman, D. *Macromolecules* **2002**, *35*, 5161.
(27) Rockford, L.; Liu, Y.; Mansky, P.; Russell, T. P.; Yoon, M.; Mochrie, S. G. J. *Phys. Rev. Lett.* **1999**, *82*, 2602.
(28) Yang, X. M.; Peters, R. D.; Nealey, P. F.; Solak, H. H.; Cerrina, F. *Macromolecules* **2000**, *33*, 9575.
(29) Rockford, L.; Mochrie, S. G. J.; Russell, T. P. *Macromolecules* **2001**, *34*, 1487.
(30) Wang, Q.; Yan, Q.; Nealey, P. F.; de Pablo, J. J. *Macromolecules* **2000**, *33*, 4512.
(31) Wang, Q.; Nath, S. K.; Graham, M. D.; Nealey, P. F.; de Pablo, J. J. *J. Chem. Phys.* **2000**, *112*, 9996.
(32) Chen, H.; Chakrabarti, A. *J. Chem. Phys.* **1998**, *108*, 6897.
(33) Petera, D.; Muthukumar, M. *J. Chem. Phys.* **1998**, *109*, 5101.
(34) Chakrabarti, A.; Chen, H. *J. Polym. Sci., Part B: Polym. Phys.* **1998**, *36*, 3127.
(35) Pereira, G. G.; Williams, D. R. M. *Macromolecules* **1999**, *32*, 758.
(36) Tsori, Y.; Andelman, D. *J. Chem. Phys.* **2001**, *115*, 1970.
(37) Groot, R. D.; Madden, T. J. *J. Chem. Phys.* **1998**, *108*, 8713.
(38) Ren, S. R.; Hamley, I. W. *Macromolecules* **2001**, *34*, 116.
(39) Fredrickson, G. H.; Ganesan, V.; Drolet, F. *Macromolecules* **2002**, *35*, 16.
(40) de Pablo, J. J.; Yan, Q.; Escobedo, F. A. *Annu. Rev. Phys. Chem.* **1999**, *50*, 377.
(41) Helfand, E.; Wasserman, Z. R. *Macromolecules* **1980**, *13*, 994.
(42) Leibler, L. *Macromolecules* **1980**, *13*, 1602.
(43) Escobedo, F. A.; de Pablo, J. J. *J. Chem. Phys.* **1996**, *105*, 4391.
(44) Binder, K.; Fried, H. *Macromolecules* **1993**, *26*, 6878.
(45) Solak, H. H.; He, D.; Li, W.; Cerrina, F. *J. Vac. Sci. Technol. B* **1999**, *17*, 3052.
(46) Peters, R. D.; Yang, X. M.; Kim, T. K.; Sohn, B. H.; Nealey, P. F. *Langmuir* **2000**, *16*, 4625.
(47) Cerrina, F., private communication.
(48) Wang, Q.; Nealey, P. F.; de Pablo, J. J. *Macromolecules* **2002**, *35*, 9563.
(49) Morkved, T. L.; Lu, M.; Urbas, A. M.; Ehrichs, E. E.; Jaeger, H. M.; Mansky, P.; Russell, T. P. *Science* **1996**, *273*, 931.
(50) Mansky, P.; DeRouchey, J.; Russell, T. P.; Mays, J.; Pitsikalis, M.; Morkved, T.; Jaeger, H. *Macromolecules* **1998**, *31*, 4399.

MA020996T